

An oligopeptide of the feline leukemia virus envelope glycoprotein is associated with morphological changes and calcium dysregulation in neuronal growth cones

AD Fails¹, TW Mitchell¹, JL Rojko² and LR Whalen¹

¹Department of Anatomy and Neurobiology, Colorado State University, Fort Collins, CO 80523, USA; ²Department of Veterinary Pathobiology, The Ohio State University, Columbus, OH 43210, USA

Neuropathogenic processes that affect the pathfinding properties of neuronal growth cones could account for many of the dysfunctions unique to retroviral infection of developing nervous systems. Pediatric HIV-1 infection, for example, is associated with a distinctive neuropathogenesis that includes marked cortical atrophy, cognitive disorders, and pyramidal dysfunction.

The ability of HIV's envelope glycoprotein, gp120, to produce increased intracellular free calcium ($[Ca^{2+}]_i$) leading to neuronal death has been documented. We hypothesize that gp120 and the envelope glycoproteins of other retroviruses may have similar calcium-increasing effects in advancing growth cones, a property which could disrupt the orderly development of the nervous system. To explore this possibility, we exposed chick ciliary ganglion neurons in culture to a known cytopathic region (CVR5) of the feline leukemia virus' envelope glycoprotein. CVR5 produced $[Ca^{2+}]_i$ increases and dose-dependent morphological changes in growth cones isolated from their cell bodies by axotomy. These responses of growth cones to CVR5 suggest that the neurotoxic effects of retroviruses could be mediated at the level of the individual growth cone through exposure to envelope glycoproteins and could constitute one mechanism by which these viruses perturb the normal development of the nervous system.

Keywords: Feline leukemia virus; feline lentiviruses; gp120 (HIV); nervous system – embryology; fluorescent microscopy

Introduction

Interest in the pathogenesis of retroviral-induced neurological disease has increased in the past decade as documentation of the neurotoxicity of retroviruses, particularly human immunodeficiency virus (HIV), has grown. The exact mechanisms by which this and other retroviruses cause injury to the nervous system are widely debated, but the neurotoxicity of HIV's envelope glycoprotein, gp120, remains the focus of much scrutiny. It has been demonstrated that application of gp120 to nervous tissue culture causes neuronal death that is associated with marked increases in free intracellular calcium ion concentrations ($[Ca^{2+}]_i$) (Dreyer *et al*, 1990; Lipton *et al*, 1991). Such increases have

been implicated as the final common pathway in a variety of neurodegenerative disorders (Choi, 1992).

Like HIV and other human retroviruses, feline retroviruses (feline leukemia virus [FeLV] and feline immunodeficiency virus [FIV]) have been associated with neurological disease, including myelopathies, behavioral abnormalities, and polyneuropathies (Hardy, 1981; Haffer *et al*, 1987; Wheeler *et al*, 1990; Hoover and Mullins, 1991; Phillips *et al*, 1994). With its predisposition to produce myelopathies and signs of long-tract disease, the neuropathology of FeLV has been compared to similar clinical syndromes associated with the human T-cell lymphotropic virus type I (HTLV-I), the retroviral cause of tropical spastic paraparesis (Hardy, 1981; Hoover and Mullins, 1991; Gessain and Gout, 1992; Hollsberg and Hafner, 1993; Nakagawa *et al*, 1995). Relative to FeLV, FIV is more likely to result in encephalopathy and other

Correspondence: AD Fails
Received 8 August 1996; revised 6 January 1997; accepted 29 January 1997

suprasegmental disturbances of function which closely resemble the neurological manifestations of HIV encephalopathy (Nathanson *et al*, 1990; Pedersen and Barlough, 1991; Hurtrel *et al*, 1992; Phillips *et al*, 1994, Portegies, 1994). These feline retroviruses may therefore provide useful models for human retroviral-induced neurologic disease.

Like gp120, the envelope glycoprotein of FeLV (gp70) confers target cell specificity upon the virus and dictates its ability to virulently infect cells. Minor variations in gp70 impart major differences in cellular tropism and pathogenicity (Hunter and Swanstrom, 1990; Hoover and Mullins, 1991; Rigby *et al*, 1992). One of the gp70's variable regions (VR5) which is thought to dictate cytotoxic proper-

ties of the virus has been isolated and sequenced. This 15-amino acid sequence as it occurs in highly cytopathic FeLV-C variants differs by only four amino acids from the sequence of the same region in an FeLV variant (FeLV-A_{Glasgow}) that exhibits low pathogenicity (Riedel *et al*, 1986; Rigby *et al*, 1992; Phipps *et al*, 1995). This variable region in a highly virulent isolate, FeLV-C_{Sarna}, has been designated CVR5; that of the same region of FeLV-A_{Glasgow} is called AVR5 (Figure 1). In its monomeric form, CVR5 has low cytopathogenicity, but when linked as an octomer to a lysine core, CVR5 becomes cytotoxic to lymphocytes in concentrations as low as 3 μ M (Phipps *et al*, 1995). CVR5 in this configuration (designated CVR5-MAP for 'multiple antigen peptide' and hereafter referred to simply as CVR5) may be presented to the cell membrane in a spatial array more like that which is seen on the surface of the intact virion, a presentation that could be essential to the physiological effect of the peptide.

Work in our laboratory demonstrated significant decreases in neuronal survival and neurite outgrowth in cultured ciliary ganglion neurons exposed to CVR5 at concentrations of 3 μ M or greater

CVR5	L	C	K	K	T	Q	K	G	H	K	G	T	H	Y	L
AVR5	•	•	N	•	•	•	Q	•	•	T	•	A	•	•	•

Figure 1 Amino acid sequences of CVR5 and AVR5.

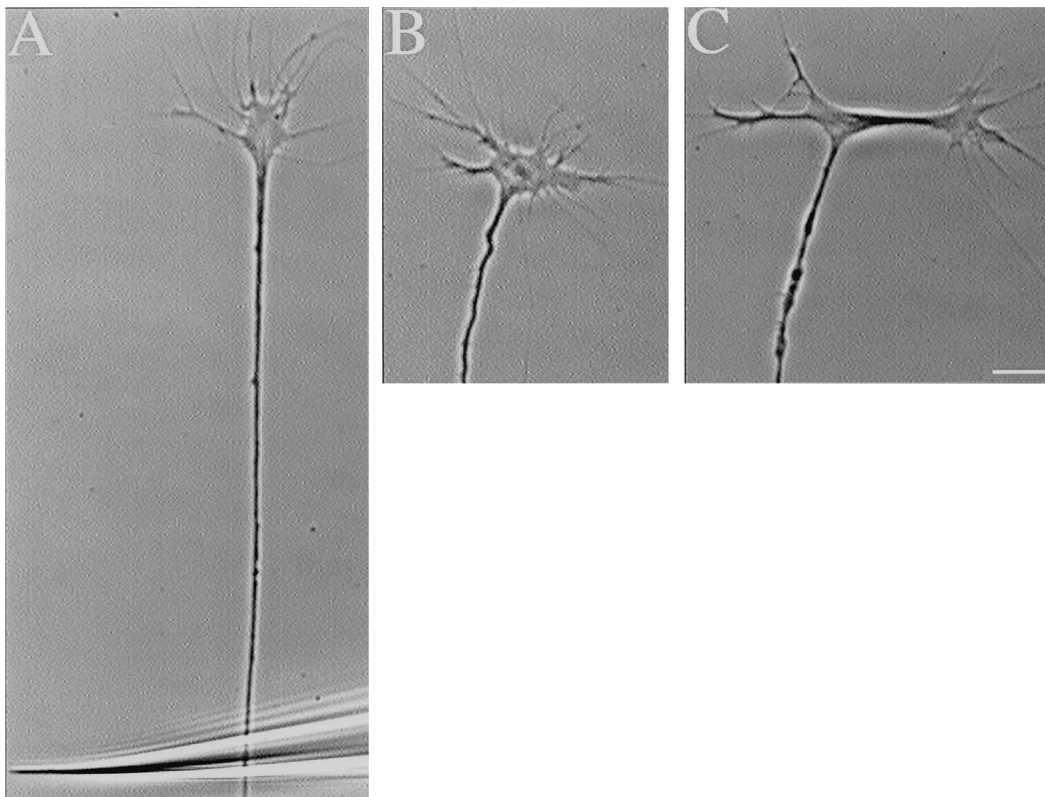


Figure 2 Effect of axotomy on a growth cone. (A) Growth cone morphology is normal prior to axotomy, with many, active filopodia and lamellipodia; tip of micropipette is seen at bottom of image. (B) 20 min following transection, the axotomized growth cone continues to exhibit normal morphology and activity. (C) 15 min later, the growth cone has branched, but its morphology is still judged to be normal based on active extension of multiple filopodia and movement of lamellipodia. Bar = 10 μ m.

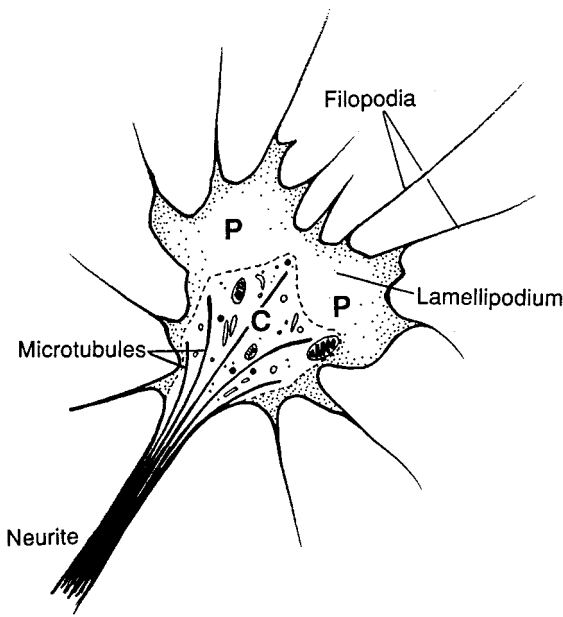


Figure 3 Diagrammatic anatomy of a normal growth cone. The peripheral zone (P) is dominated by actin cytoskeletal components and characterized by the active elaboration and retraction ('ruffling') of lamellipodia; multiple actin-based filopodia extend from the peripheral zone. The central zone (C) is the organelle-rich region of the growth cone and is dominated by microtubular components of the cytoskeleton.

(Mitchell *et al*, 1997). Additionally, neuronal $[Ca^{2+}]_i$ increased in response to CVR5 exposure, as revealed by a fluorescent calcium indicator dye, fluo-3. These findings implicate calcium dysregulation as a component of the cell injury which results from exposure to this portion of FeLV's envelope glycoprotein.

The particular aspect of retroviral disease of interest to us is the distinctive natural history of perinatal infection of the nervous system. Infants born with HIV infection are more likely to develop nervous system disease in absence of secondary infections than HIV-infected adults, i.e., as a direct viral effect. Pediatric AIDS is frequently complicated by dysfunction of motor tracts and marked cortical atrophy (Belman *et al*, 1988; Brenneman *et al*, 1990). Neurological effects of *in utero* FeLV infection of kittens is less well-documented, but congenital fetal infection and perinatal death are recognized sequelae of FeLV infection in the viremic, pregnant queen (Hoover *et al*, 1983; Hoover and Mullins, 1991).

It is our hypothesis that retroviral envelope glycoproteins can act on the developing nervous system at the level of advancing growth cones, leading to either failure to make or disruption of established neuronal connections. We investigated this hypothesis by observing the morphology and calcium regulation of the growth cones exposed to CVR5 in dissociated chick ciliary ganglion cultures.

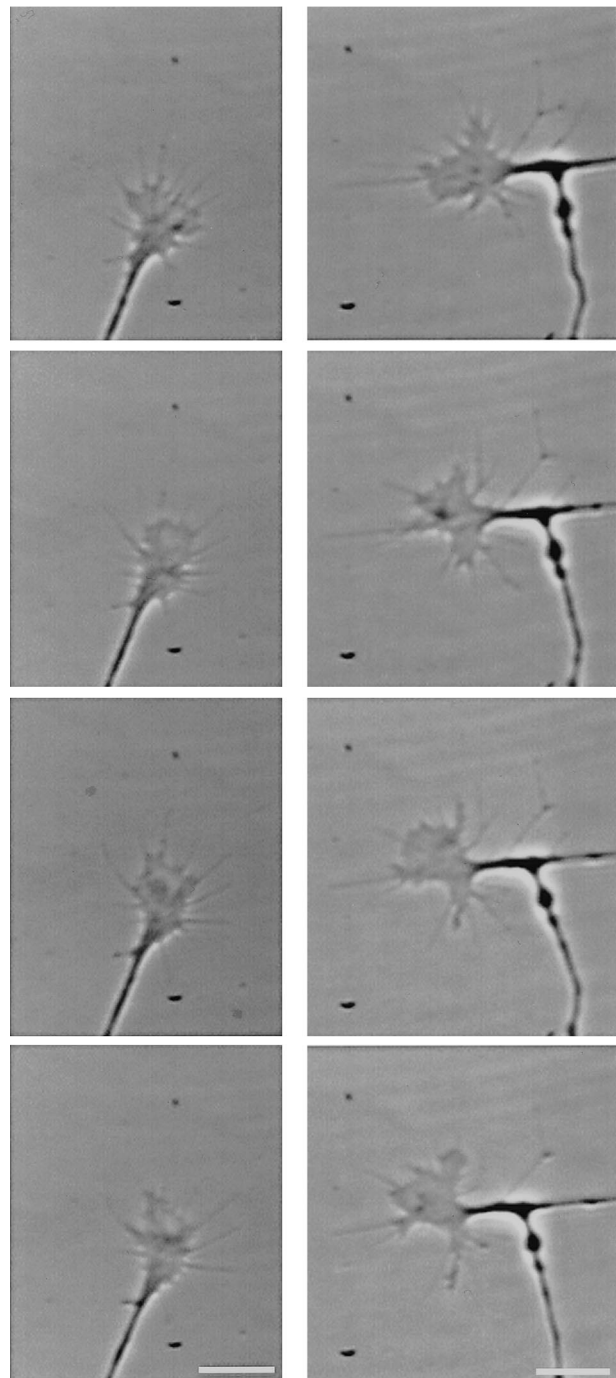


Figure 4 Phase micrographs of normal growth cones taken at 30 s intervals. On the left is an attached growth cone; growth cone on the right is axotomized. Features of normal growth cones are many long, fine filopodia and active lamellipodia. The expanded peripheral area rapidly changes shape with ruffling of lamellipodia. Bar = 10 μ m.

These cells were chosen because of (1) proven responsiveness of the cell body to CVR5, (2) the relative homogeneity of the neuronal population, and (3) the observation that anisocoria (and hence disturbance of autonomic innervation of the pupil)

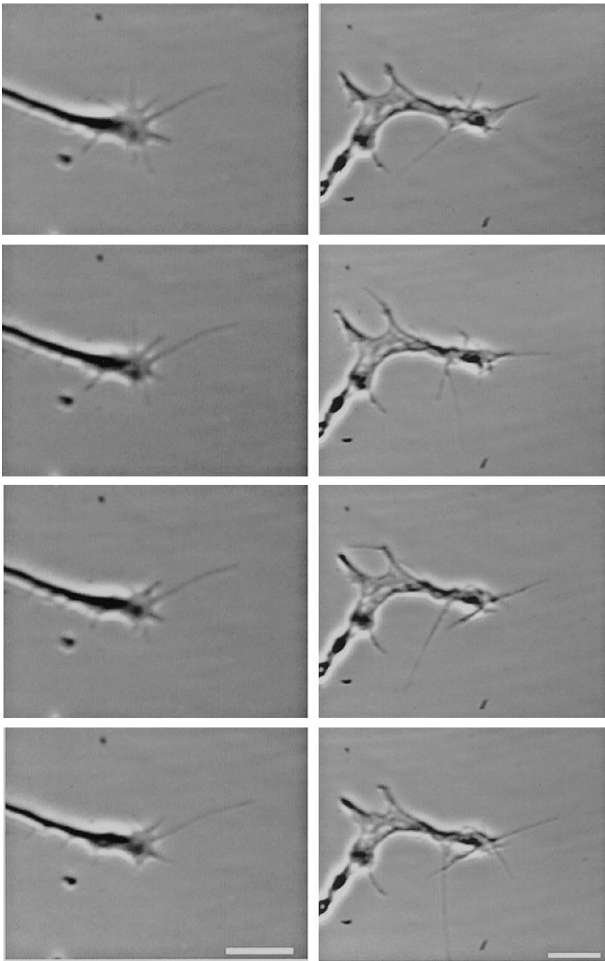


Figure 5 Phase micrographs of altered growth cones taken at 30 s intervals. On the left is an attached growth cone; growth cone on the right is axotomized. Altered growth cones have reduced numbers of filopodia, reduced filopodial and lamellipodial activity, and reduced lamellipodial area. Bar = 10 μm .

can be associated with FeLV infection (Brightman *et al*, 1977; Scagliotti, 1980). In order to isolate growth cone responses from those originating from the cell body, neurites of active growth cones were transected (axotomized). Cultures were bath-exposed to CVR5 or control solutions, and the axotomized growth cones' morphology was recorded at 15, 30, and 45 min post-treatment. In a separate set of experiments, neurons were loaded with a calcium indicator dye, fluo-3, followed by axotomy of dye-loaded growth cones. The relative fluorescence of the isolated growth cones was recorded for fifteen minutes subsequent to exposure to CVR5.

In this study, we show that CVR5 can act directly on the growth cones of cultured neurons. These actions can be manifested by changes in morphology, loss of motility, and increased $[\text{Ca}^{2+}]_i$. These effects are independent of the cell body, as they occur in growth cones that have been isolated from the soma by axotomy. This suggests a mechanism by

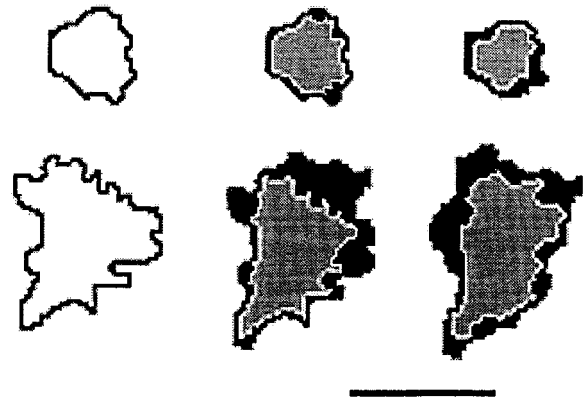


Figure 6 Difference tracings of the growth cones in left columns of Figure 4 (normal) and Figure 5 (altered). Images were generated by superimposition of consecutive frames; areas in black represent changing regions of lamellipodial expansion and retraction. The first portion of the figure corresponds to the outline of the growth cone in the first frame; the second shows area of difference between the first and second frames; the last portion of the figure shows differences between second and third frames. Note the reduced motility in the altered growth cone, whose movements are confined to small amounts of retraction over the course of 90 s. Bar = 10 μm .

which FeLV in particular and retroviruses in general might contribute to abnormal nervous system development in perinatal infections.

Results

Most growth cones (80–90%) continued to advance across the culture substrate following axotomy with a micropipette (Figure 2). Evaluation of growth cone morphology was made during the experiment by an observer blinded to the applied treatment. Each growth cone was observed in real time for a period sufficient to detect movement of filopodia and/or lamellipodia. The presence or absence of motility and the morphology was recorded, and a still image was captured for each growth cone at each observational period.

Growth cone morphology was evaluated on the basis of the following criteria: motility of filopodia and lamellipodia, number of filopodia, relative area of the P-domain (the actin-dominated cortical region comprising lamellipodia), presence of phase-dark cytoplasmic structures, and the length and density of filopodia (Figure 3). Retrospective analysis of 200 randomly selected images (100 each of normal and altered growth cones) verified the statistical difference in filopodial numbers between these two nominal categories.

'Normal' growth cones exhibited rapidly changing areas with extension, folding and retraction of long, thin filopodia. Elaboration and remodel-

ling of lamellipodia ('ruffling') was observed. This activity was readily detected over a few seconds of real time observations (Figures 4).

Growth cones interpreted as 'altered' characteristically had reduced numbers of filopodia (generally fewer than seven) which often assumed a

short, thickened appearance. Lamellipodia were reduced, and the cytoplasm frequently contained multiple phase-dark inclusions (Figure 5). All altered growth cones retained some observable motility of filopodia or lamellipodia, but this movement was less than that seen in normal growth cones (Figure 6).

Growth cones which had detached from the substrate or retracted all processes were considered 'collapsed', as were growth cones which had lost all motility when observed in real time. Collapsed growth cones usually had few or no filopodia, lacked identifiable lamellipodia, and had phase-dark intracellular accumulations (Figure 7).

Axotomized and attached growth cones underwent alteration and/or collapse in a dose-dependent fashion following bath application of CVR5. Percentages of altered and/or collapsed growth cones ('responders') among those axotomized reached statistically significant levels relative to plates treated with DMEM-HEPES at 3 ($P < 0.03$), 6 ($P < 0.004$), and 12 μM ($P < 0.0001$) CVR5 within the first 15 mins of observation and maintained significant differences throughout the observational period (Figure 8). The percentage of axotomized growth cones responding to CVR5 at 1 μM was never significantly different from control values, but was different from 12 μM ($P < 0.03$) at all time intervals. Numbers of responders among attached growth cones were significantly different relative to controls at 6 ($P < 0.006$) and 12 μM ($P < 0.0001$) CVR5 throughout the observational period (Figure 9). There was no statistically significant difference in numbers of responders between 6 and 12 μM CVR5 except for intact growth cones at 15 min, when fewer growth cones exhibited normal morphology at 12 μM than 6 μM CVR5 ($P < 0.03$). Among growth cones treated with the vehicle, DMEM-HEPES, significantly fewer axotomized than intact growth cones retained normal morphology at the end of the observational period (45 min) ($P < 0.05$). Both the rapidity of onset of alterations and the severity of changes (from mild morphological alterations to complete collapse) varied with the dose, with higher doses producing more rapid onset of more severe changes.

Three types of controls were compared to 6 μM CVR5: (1) the vehicle, HEPES-buffered DMEM, in a like volume ($n=10$), (2) 6 μM CVR5 inactivated with polyclonal antibodies ($n=5$), and (3) 6 μM AVR5 in the MAP configuration ($n=5$). The morphological responses of axotomized growth cones treated with these three controls were not statistically different from one another. There was significant difference between plates treated with 6 μM CVR5 and each of the control treatments at all time intervals examined: (1) CVR5 vs. DMEM, $P < 0.006$, (2) CVR5 vs. antibody-treated CVR5, $P < 0.03$, and (3) CVR5 vs. AVR5, $P < 0.02$ (Figure 10).

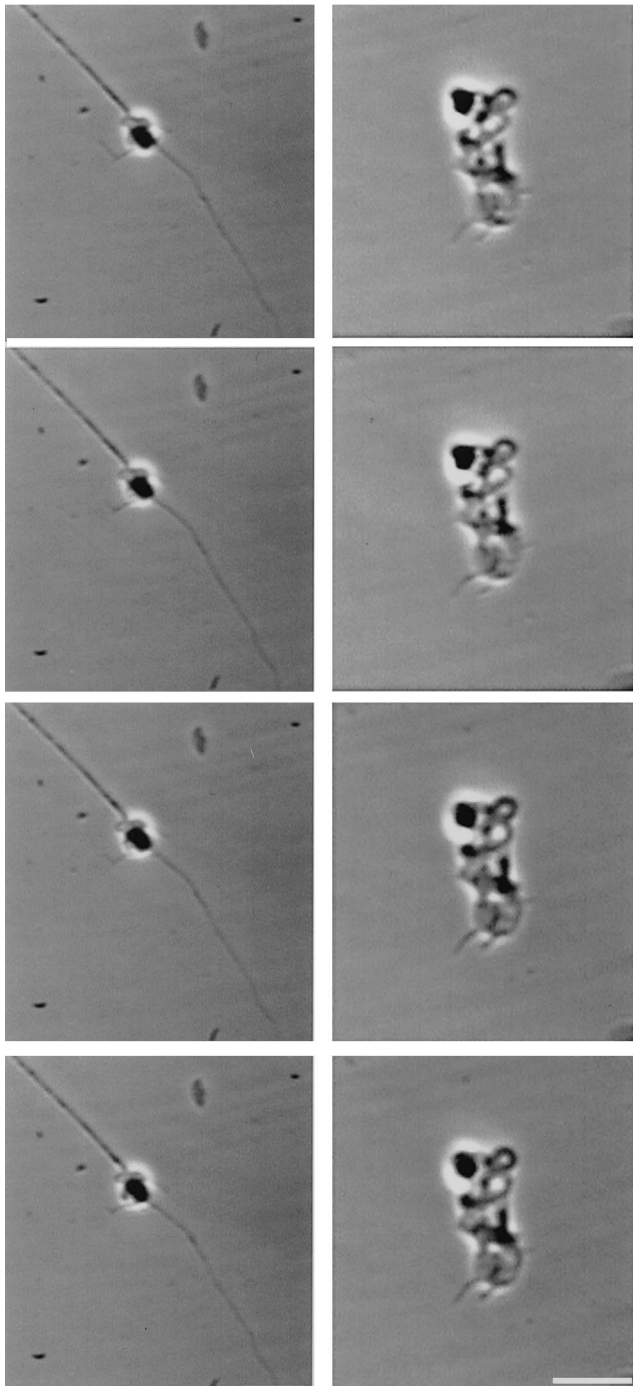


Figure 7 Phase micrographs of collapsed growth cones taken at 30s intervals. On the left is an attached growth cone; growth cone on the right is axotomized. Collapsed growth cones lack movement; there no or few filopodia, no lamellipodia, and no identifiable peripheral zone. Bar = 10 μm .

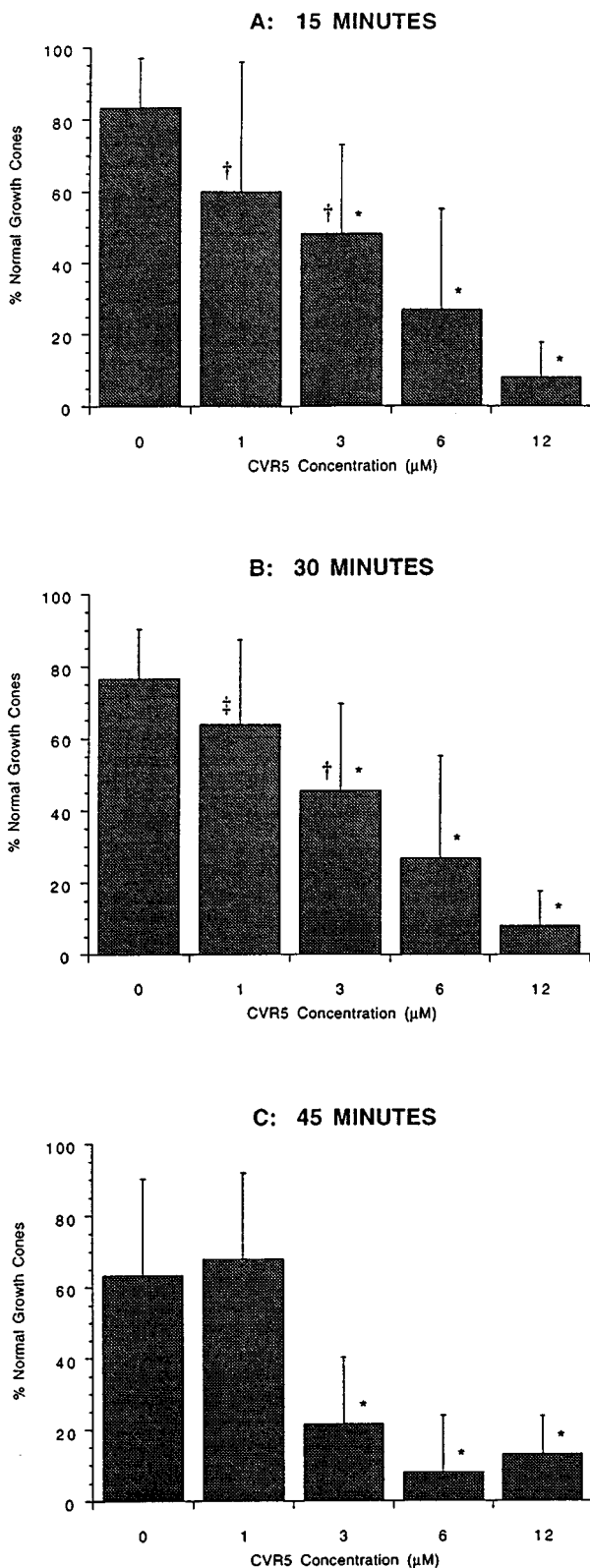


Figure 8 Percentages of axotomized growth cones exhibiting normal morphology decline with increasing doses of CVR5. (A) At 15 min post-treatment, 3, 6, and 12 μM CVR5 are significantly different from control plates (*, $P < 0.02$); 1 and 3 μM CVR5 are significantly different from 12 μM CVR5 (†, $P < 0.03$). (B) At

Fluorescence studies with fluo-3 were performed on axotomized growth cones to measure changes in $[\text{Ca}^{2+}]_i$ in response to CVR5. Growth cones which exhibited an increase of maximum fluorescence at least two standard deviations above the mean maximum fluorescence of medium-treated growth cones were judged to be 'responders'. Among growth cones treated with 1 μM CVR5, 9 out of 16 met this criterion (Figure 11). Treatment with DMEM-HEPES never increased $[\text{Ca}^{2+}]_i$. To ascertain that these control growth cones could respond with a calcium increase, 2 or 3 μM CVR5 was applied subsequent to the 20 min observation period. All controls ($n=5$) responded with an increase in fluorescence greater than two standard deviations above the mean maximum fluorescence established in the 5 minutes prior to application of CVR5 (Figure 12).

The average maximum increase in fluorescence following application of CVR5 to responding growth cones was 3.11 ± 2.14 (range: 1.63 to 6.30), whereas the average maximum increase in fluorescence following application of DMEM-HEPES to control growth cones was 1.06 ± 0.05 (range: 1.03 to 1.13) ($P < 0.05$). Control growth cones, subsequently treated with 2 or 3 μM CVR5, exhibited an average maximum fluorescence of 1.82 ± 0.34 (range: 1.42 to 2.28). This response is significantly different from the response the same growth cones exhibited after treatment with control solutions ($P < 0.003$).

Discussion

The pathfinding behavior of growth cones is essential to the development of normal connectivity of the nervous system. The process by which the active growth cone chooses one direction over another may be in some cases guided by calcium fluxes generated by receptor interactions with extracellular molecular signals (O'Connor *et al*, 1990; Kater and Mills, 1991; Letourneau *et al*, 1994). Studies of growth cones isolated from their cell bodies by axotomy have shown that these growth cones retain the ability to respond to molecular signals in the environment with increases in $[\text{Ca}^{2+}]_i$ indicating that receptors and intracellular messenger cascades exist and can function at a distance from the cell body (Rheder *et al*, 1991).

30 min post-treatment, 3, 6, and 12 μM CVR5 are significantly different from control plates (*, $P < 0.04$); 1 μM CVR5 is different from 6 and 12 μM CVR5 (†, $P < 0.02$); 3 μM CVR5 is different from 12 μM CVR5 (†, $P < 0.02$). (C) At 45 min post-treatment, 3, 6, and 12 μM CVR5 are significantly different from both control plates and 1 μM CVR5 (*, $P < 0.02$). For all concentrations and time intervals $n = 5$ culture dishes, each with 5 growth cones. 0 = DMEM.

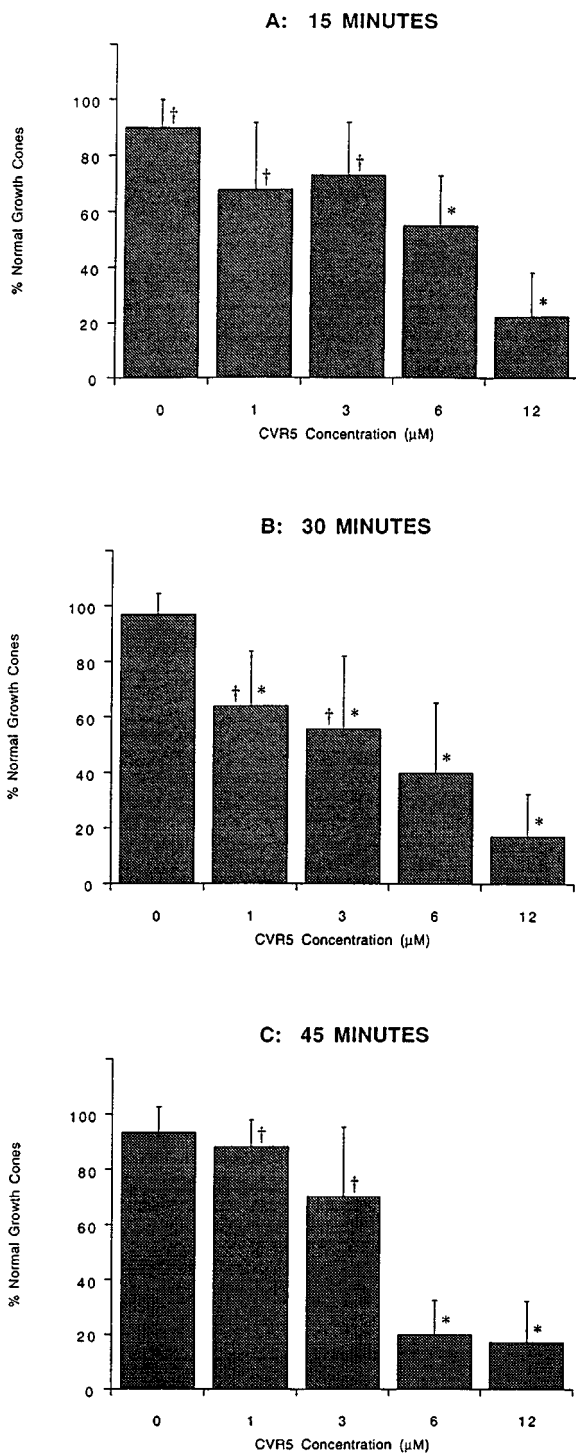


Figure 9 Percentages of attached growth cones exhibiting normal morphology decline with increasing doses of CVR5. (A) At 15 min post-treatment, 6 and 12 μM CVR5 are significantly different from plates treated with DMEM (*, $P < 0.01$); 1, 3, and 6 μM CVR5 are different from 12 μM CVR5 (†, $P < 0.03$). (B) At 30 min post-treatment, all concentrations of CVR5 are significantly different from control plates (*, $P < 0.01$); 1 and 3 μM CVR5 are significantly different from 12 μM (†, $P < 0.03$). (C) At 45 min post-treatment, 6 and 12 μM CVR5 are significantly different from control plates (*, $P < 0.001$); 1 and 3 μM CVR5 are significantly different from both 6 and from 12 μM (†,

This autonomy of the growth cone is a necessary condition of its long-distance, ‘target-seeking’ function, but may consequently render it sensitive to the presence of viral toxins. The internal free calcium ion concentration in an active growth cone is typically maintained near 200 nM (Connor, 1986); supraoptimal $[Ca^{2+}]_i$, however, can lead to collapse of the growth cone, cell dysfunction, or cell death. In this study we examined the ability of a 15-amino acid sequence from a variable region on FeLV-C’s envelope glycoprotein (CVR5) to perturb the morphology and calcium regulation of neuronal growth cones in culture.

CVR5 produces increased $[Ca^{2+}]_i$, decreased neurite outgrowth, and decreased survival in cultured chick ciliary ganglion neurons (Mitchell *et al*, 1997). To examine the responsiveness of the growth cone to this oligopeptide, we transected the neurites of active growth cones and bath-exposed the cultures to CVR5. Exposure of isolated growth cones to as little as 3 μM CVR5 produced sustained morphological alterations after 15 min. The induction of similar responses in intact neurons required exposure to 6 μM CVR5. In comparisons of intact and axotomized growth cones treated with the vehicle alone, DMEM–HEPES, a larger percentage of isolated growth cones developed abnormal morphologies following this treatment relative to identically-treated intact growth cones. It thus appears that the process of axotomy predisposes the isolated growth cone to develop abnormal morphology, even in the absence of exposure to injurious substances. Increased sensitivity to CVR5 is probably a reflection of axotomized growth cones’ reduced ability to compensate for even small perturbations of $[Ca^{2+}]_i$ homeostasis.

Fluorescence studies, performed on axotomized growth cones, showed significant increases in $[Ca^{2+}]_i$ in 56% ($n=9/16$) of growth cones exposed to 1 μM CVR5. Failure to elicit consistent calcium responses in all growth cones may be explained by three considerations. First, fluo-3-loaded growth cones were in general less likely to sustain normal morphology following axotomy than unloaded growth cones and may therefore have suffered sufficient disruption of their intracellular systems to blunt their calcium responses. Secondly, previous studies with CVR5 have described a sub-population of neurons in ciliary ganglion cell culture resistant to the $[Ca^{2+}]_i$ increasing properties of this peptide; in these cultures, 20% of the neurons did not respond with increased $[Ca^{2+}]_i$ to 12 μM CVR5 (Mitchell *et al*, 1997). Finally, the dose of CVR5 used in our calcium imaging studies

$P < 0.006$). For all concentrations and time intervals $n=5$ culture dishes, each with 5 growth cones. 0 = DMEM.

(1 μM) represents a low concentration associated with less consistent responses of neurons and growth cones. Fluorescent studies of growth cones responding to CVR5 were undertaken early in our study, prior to the majority of the morphology studies, and well before analysis of data that indicated a less consistent and robust response to 1 μM CVR5. Subsequent application of 2 or 3 μM CVR5 to control growth cones was insurance against unresponsiveness; our intent was to show that the failure of these controls to exhibit increased calcium on exposure to control solutions was not due to the inability to produce those responses when exposed to a sufficient concentration of CVR5. Studies of the dose-dependency of the calcium response were not undertaken in this series of experiments.

The number of growth cones responding with morphological changes only reached statistical significance at 3 μM CVR5; in contrast, calcium increases of greater than two standard deviations were detected in more than 50% of growth cones treated with 1 μM CVR5 and in all growth cones treated with 2 or 3 μM CVR5. This suggests that calcium responses are activated at lower concentrations than can produce observable morphological changes. Growth cones encountering low concentrations of the FeLV envelope glycoprotein *in vivo* could respond with activation of calcium-mediated second messenger systems, a response which could profoundly affect the pathfinding behavior of the growth cone.

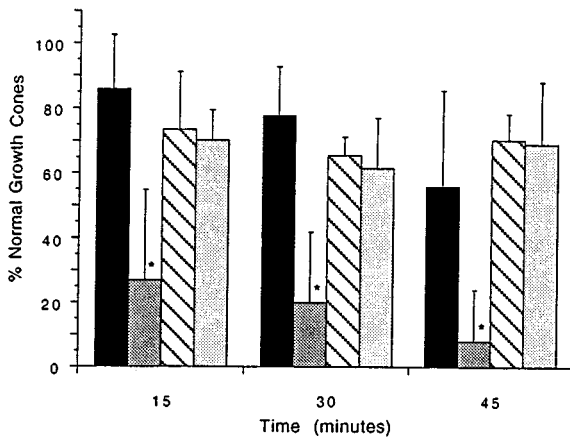


Figure 10 Percent of normal axotomized growth cones in cultures treated with HEPES-buffered DMEM (black), 6 μM CVR5 (dark grey), 6 μM CVR5 incubated with anti-CVR5 antibodies (hatched), and 6 μM AVR5 (light grey). 6 μM CVR5 is significantly different (*) from those treated with DMEM ($P < 0.006$), from those treated with 6 μM CVR5 + antibodies ($P < 0.03$), and from those treated with 6 μM AVR5 ($P < 0.02$) at all intervals. The morphological responses of growth cones treated with DMEM, those treated with 6 μM CVR5 inactivated with antibodies, and those treated with 6 μM AVR5 were not statistically different at any interval.

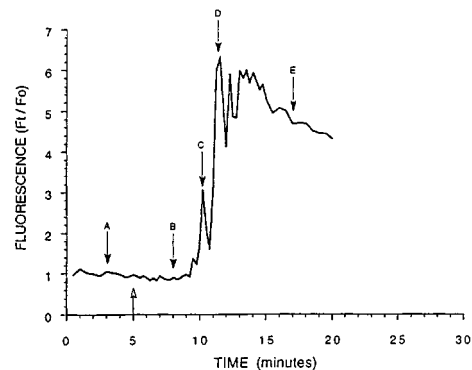
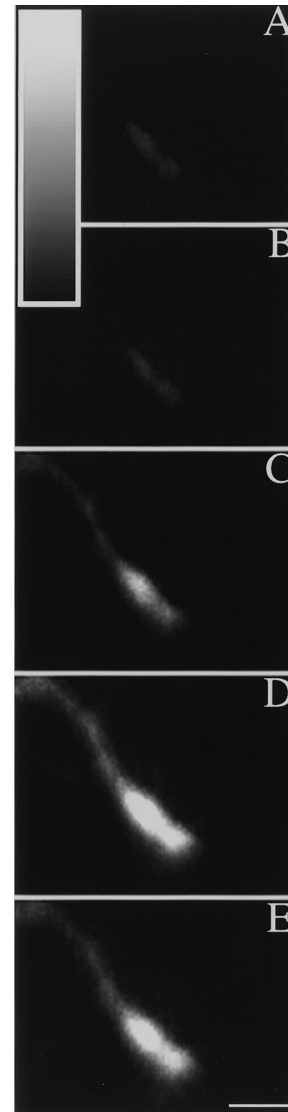
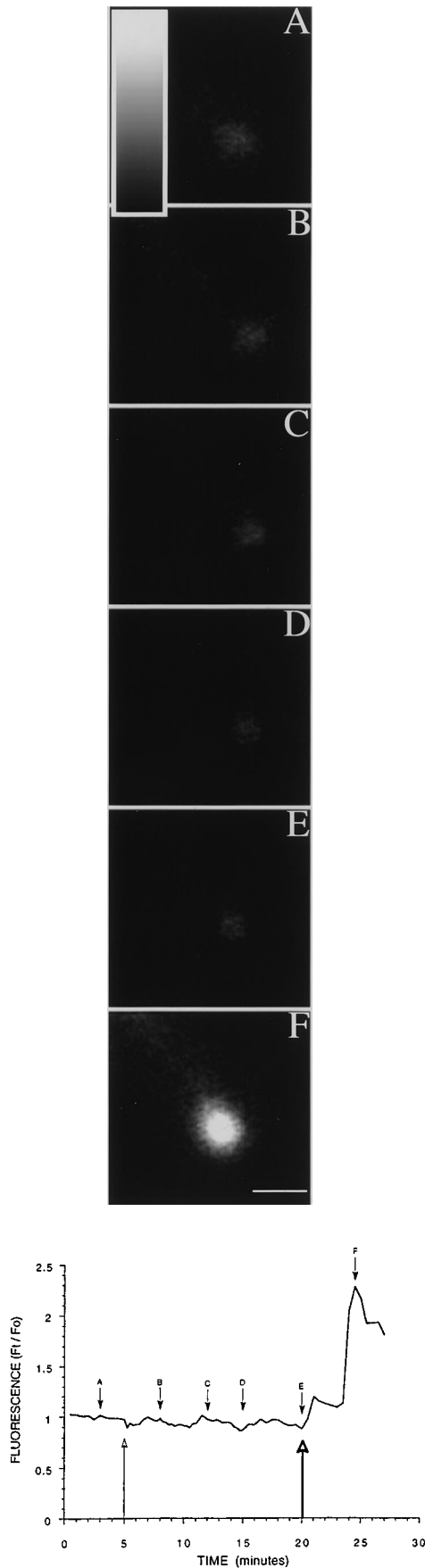


Figure 11 Relative fluorescence (open arrow) of a single growth cone treated with 1 μM CVR5 at 5 min (open arrow). Fluorescence at any given time is reported as the ratio of fluorescence at that time (F_t) to the average fluorescence (F_0) in the first 5 (pre-treatment) min. Letters on graph correspond to accompanying fluorescent micrographs; intensity of fluorescence in the growth cone is measured against the adjoining greyscale, with greatest fluorescence corresponding to the top, white portion of the greyscale. Bar = 10 μm .



Importantly, no growth cones prepared in like manner but treated with vehicle ever showed an increase in fluorescence in response to this treatment. As noted, these control growth cones were subsequently treated with 2 or 3 μM CVR5, and their ability to respond thereby established by the resulting increased $[\text{Ca}^{2+}]_i$ in all growth cones so treated. These data demonstrate a convincing link between bath exposure to CVR5 and increases in $[\text{Ca}^{2+}]_i$ within the growth cone.

The mechanism by which CVR5 elicits increased calcium in growth cones and neurons is unknown. In previous studies (Mitchell *et al*, 1997), neurons were loaded with fluo-3 then treated with CVR5 in the presence of propidium iodide. Propidium iodide undergoes a 40-fold increase in fluorescence when it enters a cell, but is highly impermeant to living membranes. Propidium iodide will therefore produce a fluorescent signal in cells only after loss of membrane integrity. Ciliary ganglion neurons responded to application of CVR5 with increases in $[\text{Ca}^{2+}]_i$ revealed by fluo-3 fluorescence, and this signal was either followed by increased propidium iodide fluorescence after a delay of 3–5 min or occurred with no subsequent propidium iodide signal. This argues against a loss of membrane integrity as the mechanism by which CVR5 produces increased intracellular free calcium in susceptible neurons. Other mechanisms by which CVR5 might elicit increases in $[\text{Ca}^{2+}]_i$ include receptor interactions and membrane depolarization. Characterization of the roles that these processes might play awaits studies with channel/receptor blockers and electrophysiological techniques.

Morphological responses reached statistical significance in axotomized growth cones at 3 μM CVR5. Calcium increases were recorded in the majority of fluo-3 loaded growth cones exposed to 1 μM CVR5. These concentrations are substantially greater than those of HIV's envelope protein, gp120, used in studies of cultured neurons (Dreyer *et al*, 1990; Lipton *et al*, 1991) and are unlikely to represent concentrations characteristic of *in vivo* infection with FeLV. This disparity between CVR5 and gp120 may represent a true difference in the calcium-perturbing power of the viral peptides, or

Figure 12 Relative fluorescence of a single growth cone treated with HEPES-buffered DMEM at 5 min (thin open arrow). Fluorescence at times between 0 and 20 min is reported as the ratio of fluorescence at that time (F_t) to the average fluorescence (F_0) in the first five (pre-treatment) min. To demonstrate its ability to respond, the growth cone was subsequently treated with 2 μM CVR5 at 20 min (thick open arrow). Fluorescence after that point is reported as the ratio between fluorescence at that time and the average fluorescence in the 5 min preceding application of CVR5 (i.e., the period from 15–20 min). Letters on graph correspond to accompanying fluorescent micrographs. Bar = 10 μm .

may be due in part to the limited resolution inherent to study of individual, isolated growth cones in our system. Detection of morphological changes in growth cones, even by quantitative assessment of criteria such as filopodial numbers or changes in growth cone area, is limited by the resolving power of the imaging system and subject to the vagaries of normal growth cone behavior and appearance. Given the highly ordered process by which the developing nervous system establishes and maintains appropriate connections between distant cells, even very small changes in growth cone steering could have major functional consequences. Inasmuch as a single filopodial contact with an attractive or repulsive molecular signal can dictate the direction of the growth cone's progress (O'Connor *et al*, 1990), contact with a restricted number of viral particles or peptides could generate a subtle intracellular signal that could substantively influence the growth cone's progress. Such signals could be well below the detection threshold of this system. We are currently undertaking studies to examine the effects of growth cone contact with CVR5 affixed to latex microbeads. This route of molecular exposure is more likely to mimic *in vivo* conditions of retroviral infection.

A number of retroviruses, including FeLV and HIV, exhibit neuropathogenicity. The envelope glycoproteins of these viruses have been implicated as important causative factors in that neurotoxicity, and have, in the cases of HIV and FeLV, been linked to intraneuronal increases in neuronal $[Ca^{2+}]_i$. The research presented here shows that an oligopeptide of FeLV's envelope glycoprotein, CVR5, is sufficient to produce both changes in morphology and increases in $[Ca^{2+}]_i$ in growth cones isolated from their somata. These findings support the hypothesis that retroviral proteins could affect the developing nervous system by disrupting the functions of neuronal growth cones and by that mechanism contribute to the nervous system dysfunction that is unique to perinatally-acquired infection.

Materials and methods

Cell culture

Ciliary ganglia were harvested from 9-day-old embryonic chicks, dissociated by incubation in 1.0 cc of 0.1% trypsin at 37°C for 25 min, then the trypsin was inactivated by addition of culture medium containing 10% fetal bovine serum. Following gentle trituration through a flame-polished glass pipette, growth medium (DMEM with 44 mM sodium bicarbonate, 10% fetal bovine serum and 2% chick eye extract (Nishi and Berg, 1981) was added to bring the suspension to approximately one ganglion per milliliter of growth medium. Dissociated cells were preplated in a 35 mm plastic culture dish for 3 h in 8.5% CO₂ at 37°C.

Culture dishes were prepared with poly-d-lysine-coated (26 $\mu\text{g}/\text{cm}^2$) no. 1 glass coverslips applied with silicon-base lubricant to the bottom of drilled plastic culture dishes. The 13 mm well of the dish was fitted with a 2–3 mm high polyethylene collar to provide a confined pool of medium in which to culture and treat cells. Prior to cell plating, laminin (3 $\mu\text{g}/\text{cm}^2$) was applied to the well and incubated for one hour before rinsing with growth medium.

Following preplating, a 300 μl aliquot of neuron-enriched supernatant was transferred to each culture dish and incubated at 37°C in 8.5% CO₂. Following removal from the incubator, bicarbonate-buffered medium was replaced with HEPES-buffered medium (DMEM with 25 mM HEPES and 10% fetal bovine serum) through five exchanges of 200 μl aliquots. Plates were coverslipped with glass and removed to a heated microscope stage (37°C). For morphology studies, neurons were viewed under phase-contrast microscopy 3 to 4 h after final plating.

For calcium studies, cells were grown for 2 h then loaded with fluo-3-AM (Molecular Probes, Inc., Eugene, Oregon) (10 μM in HEPES-buffered DMEM) for 45 min at 37°C. Plates were then rinsed with HEPES-buffered medium and transferred to the heated microscope stage for an additional 45 min of de-esterification prior to study.

CVR5 and AVR5

Lyophilized CVR5 in the MAP form was dissolved in HEPES-buffered DMEM, sterile-filtered (0.2 μm), and frozen in 50 μl aliquots representing individual culture dish treatments. Each aliquot was individually thawed at room temperature prior to application to the culture well.

In control experiments, anti-CVR5 antibodies (polyclonal, ovine) and CVR5 were incubated in HEPES-buffered DMEM at 37°C for 2 h before applying to the cultures. Anti-CVR5 antibodies were present at 0.01 mg/ml and CVR5 at 6 μM in the culture dish well's final volume of 350 μl .

In other control experiments, lyophilized AVR5 in the octomeric, lysine-linked form was similarly dissolved in HEPES-buffered DMEM. This solution was frozen into individual aliquots representing single culture dish treatments; each aliquot was individually thawed at room temperature prior to application to the culture well.

Study of growth cone morphology under phase microscopy

Morphology of growth cones was evaluated with an inverted, phase-contrast microscope (Diaphot, Nikon Corp., Tokyo, Japan) fitted with a 40 \times (0.85 N.A.) objective. Images were captured using a video camera (MIT 65, DATE-MIT, Inc., Michigan City, Indiana) and led into a video capture board in a Macintosh Quadra 700 computer for storage.

Growth cones were selected for study only if they possessed normal morphology and a neurite length of approximately 100 μm . Neurites that were crossed by others and growth cones that were likely to encounter other cells during the observation period were excluded from study. Neurites were transected (axotomized) close to the cell body using a micropipette pulled for intracellular electrophysiology and mounted on a micromanipulator. For each culture, five transected growth cones with normal post-axotomy morphology and five attached growth cones were selected for study. Morphology and motility of growth cones were evaluated in real time at 15, 30 and 45 min following bath-application of CVR5; images of the growth cones were collected at each of these time intervals. Concentrations of CVR5 used were 1, 3, 6 and 12 μM , and five culture dishes at each concentration were studied. Growth cone morphology was assessed as either 'normal' (motile filopodia extending from a growth cone with active elaboration of lamellipodia), 'altered' (reduced activity; reduction in numbers and/or blunting and thickening of filopodia; and loss of lamellipodia), or 'collapsed' (loss of activity; contraction of entire growth cone into a small, phase-dark mass; and/or loss of filopodia and lamellipodia). Motility was an important criterion by which the growth cones were assigned to a nominal category; each growth cone was viewed in real time so as to detect the movements of filopodia and ruffling of lamellipodia.

To verify that the nominal categories were supported by a quantifiable feature, analysis of filopodial numbers was undertaken. Photomicrographs of 100 growth cones judged to be normal and 100 judged to be altered were randomly selected. An observer, blinded to the original evaluation, reviewed each of these 200 images in random order, and counted the filopodia on each growth cone. In this analysis, the group originally judged to be normal bore 9.2 ± 3.2 filopodia; those originally judged to be altered had 6.0 ± 3.0 filopodia. Based on filopodial number, normal and altered growth cones were statistically different from one another ($P < 1.7 \times 10^{-11}$), confirming that analysis based on the criteria described above separated growth cones into quantifiably different categories.

Control cultures underwent one of three treatments: (1) 50 μl of HEPES-buffered DMEM ($n=6$), (2) 6 μM CVR5 incubated with anti-CVR5 antibodies ($n=5$), or (3) 6 μM AVR5. Morphology was assessed and recorded as indicated above, and images were collected.

Study of growth cones under epifluorescence

To detect alterations in growth cone $[\text{Ca}^{2+}]_i$, fluo-3-loaded, axotomized growth cones were viewed

using an inverted microscope fitted with a $40\times$ (1.3 N.A.) oil objective. A mercury light source, attenuated by neutral density filters, was used for excitation, and the illumination was limited by computer-controlled opening and closing of a shutter. Fluo-3 fluorescence was obtained using an FITC filter cube. Images were captured using an intensified charge-coupled device camera (Paultek Corp., Grass Valley, CA) and led into the video capture board in the computer. The intensity of growth cone fluo-3 fluorescence was determined using NIH Image software (version 1.59).

Fluo-3-loaded growth cones were selected and transected by the methods described above for morphology studies. A single growth cone with normal morphology (viewed through the microscope's phase optics) and low but detectable fluorescence (viewed on the camera monitor under epifluorescence) was chosen for study approximately 20 min post-axotomy to allow time for recovery from axotomy-induced calcium increases. Epifluorescent images were taken every 30 s for 5 min prior to treatment to establish a baseline level of fluorescence. Treatment consisted of either control solution (HEPES-buffered DMEM) or 1 μM CVR5. Serial images at 15 s intervals were collected for 10 min post-treatment, followed by an additional 5 min of observation at 30 s intervals. Following this observational window, control (medium-treated) growth cones were subsequently treated with 2 or 3 μM CVR5, and images collected at 15 or 30 s intervals for an additional 7 min to demonstrate the responsiveness of these control growth cones. Fluorescence at a given time (t) during the 15 min after treatment with either CVR5 or control solution was assessed as the ratio of the fluorescence at that time (F_t) divided by the average fluorescence recorded during the 5 min pre-treatment period (F_0). Fluorescence of control-treated growth cones responding to CVR5 applied at the end of the initial observational period was reported as the ratio of the fluorescence at a given time (t) divided by the average fluorescence in the 5 min immediately preceding application of CVR5.

Statistical analysis

In each culture dish, five attached and five axotomized growth cones were studied. Although no more than one growth cone was studied from any one neuron, it could be argued that the unique microenvironmental conditions within a given dish precluded absolutely random responses from the population of growth cones within that dish. To address this concern, each plate was treated as a single experimental value. Responses of all studied growth cones within that dish were averaged to produce a single data point (% responders) at each observational interval, and these averaged values were used for statistical purposes. Axotomized and intact growth cones were grouped separately for

statistical evaluation. Differences in percentage of responders at each dose were evaluated and tested for statistical significance using ANOVA.

Filopodial numbers of altered versus normal growth cones were compared using a two-tailed Student's *t*-test.

For fluorescence studies, growth cones were considered 'responders' when the maximum increase in fluorescence was greater than the mean maximum fluorescence of the post-treatment controls plus two standard deviations. Average maximum fluorescence in responding growth cones recorded following application of CVR5 and aver-

age maximum fluorescence recorded in the same period for growth cones treated with control solutions were compared using ANOVA.

Acknowledgements

This work was supported by NIH grant #RO1 NS28510 and the Colorado State University College of Veterinary Medicine and Biomedical Sciences. The authors gratefully recognize the contributions of Dr John Walrond in editing and preparing this manuscript.

References

- Belman AL, Diamond G, Dickson D, Horoupian D, Llena J, Lantos G, Rubinstein A (1988). Pediatric Acquired Immunodeficiency Syndrome. *AJDC* **142**: 29–35.
- Brenneman DE, McCune SK, Gozes Illana (1990). Acquired Immune Deficiency Syndrome and the Developing Nervous System. *Int Rev Neurobio* **32**: 305–353.
- Brightman AH, Macy DW, Gosselin Y (1977). Pupillary Abnormalities Associated with the Feline Leukemia Complex. *Fel Pract* 23–27.
- Choi DW (1992). Excitotoxic Cell Death. *J Neurobiol* **23**(9): 1261–1276.
- Connor JA (1986). Digital imaging of free calcium changes and of spatial gradients in growing processes in single, mammalian central nervous system cells. *Proc Natl Acad Sci, USA* **83**: 6179–6183.
- Dreyer EB, Kaiser PK, Offermann JT, Lipton SA (1990). HIV-1 Coat Protein Neurotoxicity Prevented by Calcium Channel Antagonists. *Science* **248**: 364–367.
- Gessain A, Gout O (1992). Chronic Myelopathy Associated with Human T-Lymphotropic Virus Type I (HTLV-I). *Ann Int Med* **117**(11): 933–946.
- Haffer KN, Sharpee RL, Beckenhauer W, Koertje WD, Fanton RW (1987). Is feline leukemia virus responsible for neurologic conditions in cats? *Vet Med* **82**: 802–805.
- Hardy WD (1981). Feline Leukemia Virus Non-Neoplastic Diseases. *JAAHA* **17**: 941–949.
- Hollberg P, Hafler DA (1993). Pathogenesis of Diseases Induced by Human Lymphotropic Virus Type I Infection. *N Eng J Med* **328**(16): 1173–1182.
- Hoover EA, Rojko JL, Quackenbush SL (1983). Congenital Feline Leukemia Virus Infection. *Leuk Rev Internat* **1**: 7–8.
- Hoover EA, Mullins JI (1991). Feline leukemia virus infection and diseases. *JAVMA* **199**(10): 1287–1297.
- Hunter E, Swanstrom R (1990). Retrovirus Envelope Glycoproteins. *Curr Top Microbio Immuno* **157**: 187–253.
- Hurtel M, Ganiere J-P, Guelfi J-F, Chakrabarti L, Maire M-A, Gray F, Montagnier L, Hurtel B (1992). Comparison of early and late feline immunodeficiency virus encephalopathies. *AIDS* **6**: 399–406.
- Kater SB, Mills LR (1991). Regulation of Growth Cone Behavior by Calcium. *J Neurosci* **11**(4): 891–899.
- Letourneau PC, Snow DM, Gomez TM (1994). Growth cone motility: substratum-bound molecules, cytoplasmic $[Ca^{2+}]$ and Ca^{2+} -regulated proteins. *Prog Brain Res* **102**: 35–48.
- Lipton SA, Sucher NJ, Kaiser PK, Dreyer EB (1991). Synergistic Effects of HIV Coat Protein and NMDA Receptor-Mediated Neurotoxicity. *Neuron* **7**: 111–118.
- Mitchell TW, Rojko JL, Hartke JR, Mihajlov AR, Kasameyer GA, Gasper PW, Whalen LR (1997). FeLV envelope protein (gp70) variable region 5 causes alterations in calcium homeostasis and toxicity of neurons. *AIDS Res Hum Retrovirus* (in press).
- Nakagawa M, Izumo S, Ijichi S, Kubota H, Arimura K, Kawabata M, Osame M (1995). HTLV-1-associated myelopathy: analysis of 213 patients based on clinical features and laboratory findings. *J Neurovir* **1**(1): 50–61.
- Nathanson N, Cook DG, Kolson DL, Gonzalez-Scarano F (1990). Pathogenesis of HIV Encephalopathy. *Ann N Y Academy Sci* **724**: 87–106.
- Nishi R, Berg DK (1981). Two components from eye tissue that differentially stimulate the growth and development of ciliary ganglion neurons in cell culture. *J Neurosci* **1**(5): 505–513.
- O'Connor TP, Duerr JS, Bentley D (1990). Pioneer Growth Cone Steering Decisions Mediated by Single Filopodial Contacts *in situ*. *J Neurosci* **10**(12): 3935–3946.
- Pedersen NC, Barlough JE (1991). Clinical overview of feline immunodeficiency virus. *JAVMA* **199**(10): 1298–1305.
- Phillips TR, Prospero-Garcia O, Puaoli DL, Lerner DL, Fox HS, Olmsted RA, Bloom FE, Henriksen SJ, Elder JH (1994). Neurological abnormalities associated with feline immunodeficiency virus infection. *J Gen Virol* **75**: 979–987.
- Phipps AJ, Harke JR, Mathes LE, Rojko JL (1995). Apoptosis Induction Via Variable Region 5 of the FeLV-CSarma Envelope Glycoprotein: A Feline Model of Retroviral Apoptosis Induction. (abstr) *J Cell Biochem Suppl* **21B**: 241.
- Portegies P (1994). AIDS Dementia Complex: A Review. *JAIDS* **7** (Suppl. 2) S38–S49.



- Rehder V, Jensen JR, Dou P, Kater SB (1991). A Comparison of Calcium Homeostasis in Isolated and Attached Growth Cones of the Snail *Helisoma*. *J Neurobio* **22(5)**: 499–511.
- Riedel N, Hoover EA, Gasper PW, Nicolson MO, Mullins JI (1986). Molecular Analysis and Pathogenesis of the Feline Aplastic Anemia Retrovirus, Feline Leukemia Virus C-SARMA. *J Virol* **60(1)**: 242–250.
- Rigby MA, Rojko JL, Stewart MA, Kociba GJ, Cheney CM, Rezanka LJ, Mathes LE, Hartke JR, Jarrett O, Neil JC (1992). Partial dissociation of subgroup C phenotype and *in vivo* behavior in feline leukaemia viruses with chimeric envelope genes. *J Gen Virol* **73**: 2839–2847.
- Scagliotti RH (1980). Current Concepts in Veterinary Neuro-Ophthalmology. *Vet Clin N Amer* **10(2)**: 417–436.
- Wheeler DW, Whalen LR, Gasper PW, *et al* (1990). A feline model of the AIDS dementia complex (ADC)? (abstr) Proceedings, 6th Intl Conf on AIDS, 190.